

Radiative decays of bottomonia into charmonia and light mesons

Ying-Jia Gao ^(a), Yu-Jie Zhang ^(a), and Kuang-Ta Chao ^(a)

^(a) *Department of Physics, Peking University, Beijing 100871, People's Republic of China*

In the framework of nonrelativistic QCD, we study the radiative decays of bottomonia into charmonia, including $\Upsilon \rightarrow \chi_{cJ}\gamma$, $\Upsilon \rightarrow \eta_c\gamma$, $\eta_b \rightarrow J/\psi\gamma$, and $\chi_{bJ} \rightarrow J/\psi\gamma$. We give predictions for their branching ratios with numerical calculations. E.g., we predict the branching ratio for $\eta_b \rightarrow J/\psi\gamma$ is about 1×10^{-7} . As a phenomenological model study, we further extend our calculation to the radiative decays of bottomonia into light mesons by assuming the $f_2(1270)$, $f'_2(1525)$ and other light mesons to be described by nonrelativistic $q\bar{q}$ ($q = u, d, s$) bound states with constituent quark masses. The calculated branching ratios for $\Upsilon \rightarrow f_2(1270)\gamma$ and $\Upsilon \rightarrow f'_2(1525)\gamma$ are roughly consistent with the CLEO data. Comparisons with radiative decays of charmonium into light mesons such as $J/\psi \rightarrow f_2(1270)\gamma$ are also given. In all calculations the QED contributions are taken into account and found to be significant in some processes.

PACS numbers: 12.38.Bx; 13.25.Hw; 14.40.Gx

I. INTRODUCTION

Radiative decays of bottomonium (e.g. Υ , η_b , χ_{bJ}) into charmonium are expected to be described by nonrelativistic quantum chromodynamics (NRQCD), since both bottomonium and charmonium are made of heavy quark and heavy antiquark, and are nonrelativistic bound states. For heavy quarkonium decay and production, the rates can be factorized into a short-distance part, which can be calculated in QCD perturbatively, and a long-distance part, which are governed by nonperturbative QCD dynamics [1]. Therefore, radiative decays of bottomonium into charmonium may provide a useful test for NRQCD factorization, which is assumed to hold also for these specific exclusive processes, and may also provide some practical estimates for decays such as $\eta_b \rightarrow J/\psi\gamma$, which might be useful in search for the not yet discovered η_b meson. As a phenomenological model study, we further extend our calculation to the radiative decays of bottomonia into light mesons by assuming the $f_2(1270)$, $f'_2(1525)$ and other light mesons to be described by nonrelativistic $q\bar{q}$ ($q = u, d, s$) bound states with constituent quark masses m_q ($q = u, d$) = 350 MeV, $m_s = 500$ MeV as in constituent quark models. These radiative decays are known as the gluon rich channels, and regarded as a good place to investigate the interactions between quarks and gluons in these OZI forbidden processes, and there have been some earlier work discussing these processes (see, e.g., [2, 3]). In this paper, as our previous work [4], we will perform a complete numerical calculation for the quark-gluon loop diagrams involved in these processes, and we will also include contributions from QED diagrams in the same processes.

We adopt the assumption that both heavy quarkonium and light mesons are described by the color-singlet non-relativistic wave functions. Based on this assumption, we study $\Upsilon \rightarrow \chi_{cJ}\gamma$, $\Upsilon \rightarrow \eta_c\gamma$, $\Upsilon \rightarrow f_J\gamma$, $\Upsilon \rightarrow \eta\gamma$, $J/\psi \rightarrow f_J\gamma$, $J/\psi \rightarrow \eta\gamma$, $\chi_{bJ} \rightarrow J/\psi(\rho, \omega, \phi)\gamma$ and $\eta_b \rightarrow J/\psi(\rho, \omega, \phi)\gamma$ etc.

The rest of this paper is as follows. In section II, we will give the descriptions and main techniques in our calculations, and then make predictions for the decay rates of $\Upsilon \rightarrow \chi_{cJ}\gamma$, $\Upsilon \rightarrow \eta_c\gamma$, $\eta_b \rightarrow J/\psi\gamma$, and $\chi_{bJ} \rightarrow J/\psi\gamma$. Then, in the following section, we will generalize this method to those processes in which the final states are light mesons. Finally, we will summarize all the results in section IV.

II. BOTTOMONIUM RADIATIVE DECAYS TO CHARMONIUM

In this section, we will study the radiative decays of bottomonium into charmonium. In NRQCD, heavy quarkonium wave function is described by a Fock state expansion in terms of the relative velocity v between the quark and antiquark, and the leading term is a color-singlet $Q\bar{Q}$ state, which has the same quantum numbers as the physical heavy quarkonium. In certain processes, the non-leading terms with color-octet $Q\bar{Q}$ pair and soft gluons may make dominant contributions. E.g., in the Υ radiative decays to light quark jets $\Upsilon \rightarrow q\bar{q}\gamma$ the color-octet contribution could be larger than the color-singlet contribution (depending on the estimates of the color-octet matrix elements) [5]. In the radiative decays of bottomonium into charmonium, the short distance transitions of a color-octet $b\bar{b}$ into a color-octet $c\bar{c}$ by emitting a photon are shown in Fig.1, where $q = c$, and $q\bar{q}$ are in color-octet (3S_1)⁸ or (3P_J)⁸. Compared with the case of Υ radiative decays to light quark jets $\Upsilon \rightarrow q\bar{q}\gamma$ (see Ref.[5] for an estimate of the color-octet contributions),

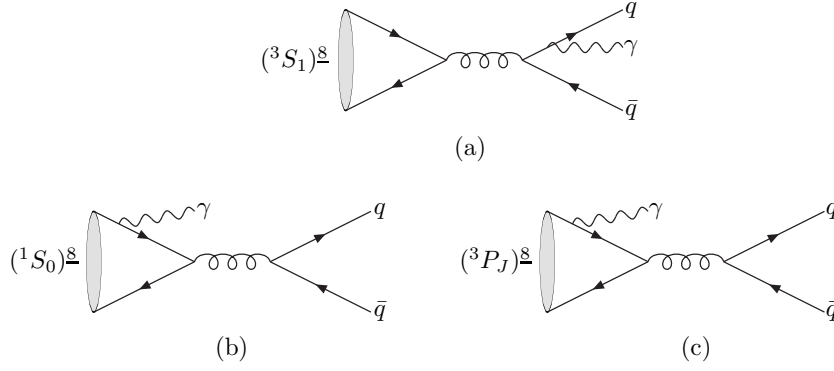


FIG. 1: Feynman diagrams for transitions from color octet $b\bar{b}$ to color-octet $q\bar{q}$ (where $q = c$) by emitting a photon

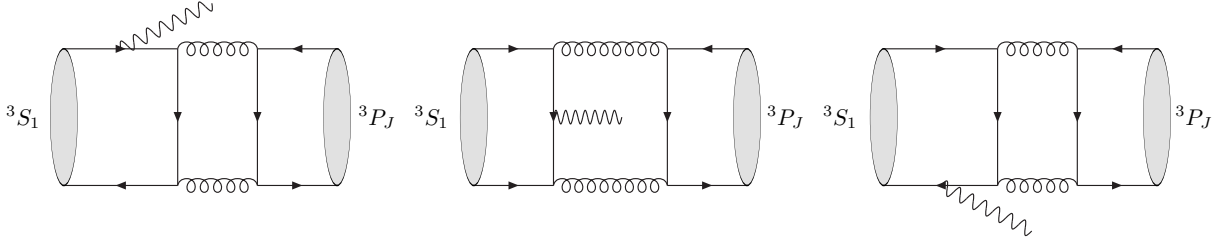


FIG. 2: Typical QCD Feynman diagrams for heavy quarkonium (3S_1) radiative decays into (3P_J) mesons

here the contribution of color-octet $c\bar{c}$ is greatly suppressed by the smallness of the color-octet matrix elements of $({}^3S_1)^8$ or $({}^3P_J)^8$ (note that the color-octet matrix element of $({}^3S_1)^8$ is only 1% of that of color-singlet $({}^3S_1)^1$ for J/ψ). Therefore, we will neglect the color-octet contributions, and only concentrate on the color-singlet description of heavy quarkonia in the following calculations.

A. General results

In the nonrelativistic approximation, the Υ radiative decay into a color-singlet $c\bar{c}$ pair, which subsequently hadronizes into charmonium, can be described by the diagrams in Fig.2, and the amplitude can be expressed as[6]

$$\begin{aligned}
\mathcal{A}\left(b\bar{b}({}^3S_1)(2p_b) \rightarrow c\bar{c}({}^{2S+1}L_J)(2p_c)\right) &= \sqrt{C_{L\Upsilon}}\sqrt{C_L} \sum_{L\Upsilon_z S\Upsilon_z} \sum_{s_1 s_2} \sum_{jk} \sum_{L_z S_z} \sum_{s_3 s_4} \sum_{il} \\
&\times \langle 1 | \bar{3}k; 3j \rangle \langle J_\Upsilon J_{\Upsilon_z} | L_\Upsilon L_{\Upsilon_z}; S_\Upsilon S_{\Upsilon_z} \rangle \langle S_\Upsilon S_{\Upsilon_z} | s_1; s_2 \rangle \\
&\times \langle s_3; s_4 | S S_z \rangle \langle L L_z; S S_z | J J_z \rangle \langle 3l; \bar{3}i | 1 \rangle \\
&\times \begin{cases} \mathcal{A}\left(b_j(p_b) + \bar{b}_k(p_b) \rightarrow \gamma(p_3) + c_l(p_c) + \bar{c}_i(p_c)\right) & (L = S), \\ \epsilon_\alpha^*(L_Z) \mathcal{A}^\alpha\left(b_j(p_b) + \bar{b}_k(p_b) \rightarrow \gamma(p_3) + c_l(p_c) + \bar{c}_i(p_c)\right) & (L = P), \end{cases} \quad (1)
\end{aligned}$$

where $\langle 3l; \bar{3}i | 1 \rangle = \delta_{li}/\sqrt{N_c}$, $\langle s_1; s_2 | S S_z \rangle$, and $\langle L L_z; S S_z | J J_z \rangle$ are respectively the color-SU(3), spin-SU(2), and angular momentum Clebsch-Gordan coefficients for $Q\bar{Q}$ pairs projecting on appropriate bound states. $\mathcal{A}(b_j(p_b) + \bar{b}_k(p_b) \rightarrow Q_l(p_c) + \bar{Q}_i(p_c))$ is the decay amplitude for $Q\bar{Q}$ production and \mathcal{A}^α is the derivative of the amplitude with respect to the relative momentum between the quark and anti-quark in the bound state. The coefficients $C_{L\Upsilon}$ and C_L can be related to the radial wave function of the bound states or its derivative with respect to the relative spacing as

$$C_S = \frac{1}{4\pi} |R_s(0)|^2, \quad C_P = \frac{3}{4\pi} |R'_p(0)|^2. \quad (2)$$

The spin projection operators $P_{SS_z}(p, q)$ which describe production of quarkonium are expressed in terms of quark

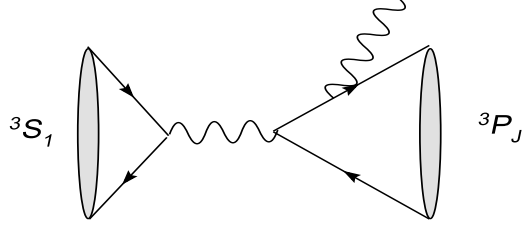


FIG. 3: Typical QED Feynman diagrams for heavy quarkonium (3S_1) radiative decays into (3P_J) mesons

and anti-quark spinors as[6, 7]:

$$P_{SS_z}(p, q) = \sum_{s_1, s_2} v\left(\frac{p}{2} - q, s_2\right) \bar{u}\left(\frac{p}{2} + q, s_1\right) \langle s_1; s_2 | SS_z \rangle, \quad (3)$$

We list the spin projection operators and their derivatives with respect to the relative momentum, which will be used in the calculations, as

$$P_{00}(p, 0) = \frac{1}{2\sqrt{2}} \gamma_5 (\not{p} + 2m), \quad (4)$$

$$P_{1S_z}(p, 0) = \frac{1}{2\sqrt{2}} \not{\epsilon}^*(S_z) (\not{p} + 2m), \quad (5)$$

$$P_{1S_z}^\alpha(p, 0) = \frac{1}{4\sqrt{2}m} [\gamma^\alpha \not{\epsilon}^*(S_z) (\not{p} + 2m) - (\not{p} - 2m) \not{\epsilon}^*(S_z) \gamma^\alpha]. \quad (6)$$

And the spin projection operators which describe the annihilation of quarkonium are the complex conjugate of the corresponding operators for production. The polarization vectors for the 3P_J states are shown below:

$$\sum_{L_z S_z} \epsilon^{*\alpha(L_z)} \epsilon^{*\beta(S_z)} \langle 1L_z; 1S_z | 1J_z \rangle = \frac{-i\epsilon^{\alpha\beta\lambda\kappa} p_\kappa \epsilon_\lambda^*(J_z)}{\sqrt{2}M}, \quad (7)$$

$$\sum_{L_z S_z} \epsilon^{*\alpha(L_z)} \epsilon^{*\beta(S_z)} \langle 1L_z; 1S_z | 00 \rangle = \frac{1}{\sqrt{3}} \left(-g^{\alpha\beta} + \frac{p^\alpha p^\beta}{M^2} \right), \quad (8)$$

$$\sum_{L_z S_z} \epsilon^{*\alpha(L_z)} \epsilon^{*\beta(S_z)} \langle 1L_z; 1S_z | 2J_z \rangle = \epsilon^{*\alpha\beta}(J_z), \quad (9)$$

where p is the momentum of P-wave quarkonium, and M is the mass of the corresponding quarkonium. $\epsilon_\lambda(J_z)$ are the polarization vectors for $J = 1$. $\epsilon^{\alpha\beta}(J_z)$ are the polarization vectors for $J = 2$, which are symmetric under the exchange $\alpha \leftrightarrow \beta$.

The QCD Feynman diagrams of $\Upsilon \rightarrow \gamma \eta_c(\chi_{cJ})$, in which the $c\bar{c}$ are produced through gluons, are shown in FIG.2, while the QED Feynman diagrams, in which the $c\bar{c}$ are produced through the photon, are shown in FIG.3. In the calculation, we use `FeynCalc` [8] for the tensor reduction and `LoopTools`[9] for the numerical evaluation of infrared safe integrals. We follow the way in Ref.[10] to deal with five-point functions and high tensor loop integrals that can not be calculated by `LoopTools` and `FeynCalc`, such as

$$E_{\alpha\beta\rho\sigma} = \int d^D k \frac{k_\alpha k_\beta k_\rho k_\sigma}{k^2 [(k+p_c)^2 - m_c^2] (k+2p_c)^2 [(p_b+k)^2 - m_b^2] [(k+2p_c-p_b)^2 - m_b^2]}. \quad (10)$$

where p_c is the momentum of c quark, p_b the momentum of b quark, m_c the charm quark mass, and m_b the bottom quark mass.

In the numerical calculations, the quark masses are taken to be $m_b = 4.7$ GeV, $m_c = 1.5$ GeV, the wave functions at the origin can be found from potential model calculations in Ref.[11]: $|\mathcal{R}_S^{bb}(0)|^2 = 6.477$ GeV³, $|\mathcal{R}_S^{c\bar{c}}(0)|^2 = 0.81$ GeV³, $|\mathcal{R}_P^{bb}(0)|^2 = 1.417$ GeV⁵, $|\mathcal{R}'^{c\bar{c}}_P(0)|^2 = 0.075$ GeV⁵. In the bottomonium decay, the strong coupling constant is chosen as $\alpha_s(2m_b) = 0.19$. The numerical results of radiative decays of bottomonium into charmonium are listed in Table I.

process	$\Upsilon \rightarrow \chi_{c2}\gamma$	$\Upsilon \rightarrow \chi_{c1}\gamma$	$\Upsilon \rightarrow \chi_{c0}\gamma$	$\Upsilon \rightarrow \eta_c\gamma$
BR_{QCD}	5.1×10^{-6}	4.5×10^{-6}	4.0×10^{-6}	2.9×10^{-5}
$BR_{QCD+QED}$	5.6×10^{-6}	9.8×10^{-6}	3.2×10^{-6}	4.9×10^{-5}
process	$\chi_{b2} \rightarrow J/\psi\gamma$	$\chi_{b1} \rightarrow J/\psi\gamma$	$\chi_{b0} \rightarrow J/\psi\gamma$	$\eta_b \rightarrow J/\psi\gamma$
$\Gamma_{QCD}(\text{GeV})$	2.7×10^{-10}	3.8×10^{-10}	5.0×10^{-10}	2.8×10^{-9}
$\Gamma_{QCD+QED}(\text{GeV})$	3.6×10^{-10}	3.7×10^{-10}	1.3×10^{-10}	9.6×10^{-10}
$\Gamma_{QED}(\text{GeV})$	3.8×10^{-11}	3.3×10^{-12}	1.3×10^{-10}	1.2×10^{-9}

TABLE I: Decay widths and branching ratios for radiative decays of bottomonium into charmonium. The decay widths Γ are in units of GeV, and the branching ratios BR are given for the Υ .

B. η_b radiative decay to J/ψ

The η_b meson is the only one among the low lying bottomonium states that has not been observed experimentally. To search for the η_b meson a number of decay channels have been suggested, e.g., decays into the $J/\psi J/\psi$ and $D\bar{D}^{(*)}$ [15, 16, 17]. In any case, the radiative decay $\eta_b \rightarrow J/\psi\gamma$ should be a useful channel for the η_b in view of the cleanness of the signal (this possibility has also been considered in Ref.[18]).

From Table I, we can see that for the η_b decay $\eta_b \rightarrow J/\psi\gamma$ the QCD and QED contributions are comparable but destructive, and, as a result, the decay width of $\eta_b \rightarrow J/\psi\gamma$ is only 9.6×10^{-10} GeV. In order to know the branching ratio of this decay channel, we should have an estimate for the η_b total width. In fact, we can estimate its total width through $\Gamma_{tot}(\eta_b) \approx \Gamma(\eta_b \rightarrow gg)$ [1]. For $\Gamma(\eta_b \rightarrow gg)$, with next to leading order (NLO) QCD radiative corrections, we have

$$\Gamma(\eta_b \rightarrow gg) = \frac{|\mathcal{R}_s(0)|^2 C_F \alpha_s^2 (2m_b)}{2m_b^2} \left\{ 1 + \left[\left(\frac{\pi^2}{4} - 5 \right) C_F + \left(\frac{199}{18} - \frac{13\pi^2}{24} \right) C_A - \frac{8}{9} n_f \right] \frac{\alpha_s}{\pi} \right\}. \quad (11)$$

With the parameters used above, we can get $\Gamma_{tot}(\eta_b) \approx 11.4$ MeV. Then the branching ratio is $Br(\eta_b \rightarrow \gamma J/\psi) \approx 8.4 \times 10^{-8}$. If we use the leading order formula in Eq.(11), the decay width is $\Gamma_{tot}(\eta_b) \approx 7.1$ MeV, and the branching ratio becomes $Br(\eta_b \rightarrow \gamma J/\psi) \approx 1.4 \times 10^{-7}$.

On the other hand, with the spin symmetry in the nonrelativistic limit ($v = 0$), the η_b wave function at the origin $|\mathcal{R}_s(0)|^2$ can be determined from the Υ leptonic width,

$$\Gamma(\Upsilon \rightarrow e^+e^-) = N_c Q_b^2 \alpha^2 \frac{|\mathcal{R}_s(0)|^2}{3m_b^2} \left(1 - \frac{16\alpha_s}{3\pi} \right), \quad (12)$$

and the η_b total width is then related to the Υ leptonic width,

$$\Gamma_{tot}(\eta_b) = \frac{3C_F \alpha_s^2 (2m_b)}{2N_c Q_b^2 \alpha^2} \frac{1 + \left[\left(\frac{\pi^2}{4} - 5 \right) C_F + \left(\frac{199}{18} - \frac{13\pi^2}{24} \right) C_A - \frac{8}{9} n_f \right] \frac{\alpha_s}{\pi}}{1 - \frac{16\alpha_s}{3\pi}} \Gamma(\Upsilon \rightarrow e^+e^-). \quad (13)$$

Using $m_b = 4.7$ GeV, $\alpha_s(2m_b) = 0.19$, and experimental data $\Gamma(\Upsilon \rightarrow e^+e^-) = 1.340 \pm 0.018$ KeV[14], we can get $\Gamma_{tot}(\eta_b) \approx 13.0$ MeV. Then the branching ratio is $Br(\eta_b \rightarrow \gamma J/\psi) \approx 7.3 \times 10^{-8}$. If we use the leading order formula in Eq.(11) and Eq.(12), the $\Gamma_{tot}(\eta_b) \approx 5.45$ MeV, the branching ratio is $Br(\eta_b \rightarrow \gamma J/\psi) \approx 1.7 \times 10^{-7}$.

In any case, we find that the branching ratio $Br(\eta_b \rightarrow \gamma J/\psi)$ is of order 1×10^{-7} . This small number makes it quite difficult to search for η_b through this decay channel.

C. Helicity ratios with χ_{c1} and χ_{c2}

We give predictions for branching ratios for different helicity states in $\Upsilon \rightarrow \chi_{cJ}\gamma$ decays. As in Ref. [12], we choose the moving direction of χ_{cJ} as the z-axis, and introduce three polarization vectors:

$$\begin{aligned} \omega^\mu(1) &= \frac{-1}{\sqrt{2}}(0, 1, i, 0), \\ \omega^\mu(-1) &= \frac{1}{\sqrt{2}}(0, 1, -i, 0) \\ \omega^\mu(0) &= \frac{1}{m}(|\mathbf{k}|, 0, 0, k^0), \end{aligned} \quad (14)$$

	QCD	QCD+QED		QCD	QCD+QED
$x^2(\Upsilon \rightarrow \gamma\chi_{c2})$	0.37	0.38	$x^2(\Upsilon \rightarrow \gamma\chi_{c1})$	0.064	0.075
$y^2(\Upsilon \rightarrow \gamma\chi_{c2})$	0.14	0.14			

TABLE II: Results for $\Upsilon \rightarrow \chi_{cJ}\gamma (J = 1, 2)$ with different helicity states

thus we can characterize the tensor $\epsilon^{\mu\nu}(\lambda)$ of χ_{c2}

$$\begin{aligned}
\epsilon^{\alpha\beta}(2) &= \omega^\alpha(1)\omega^\beta(1) \\
\epsilon^{\alpha\beta}(1) &= \frac{1}{\sqrt{2}}(\omega^\alpha(1)\omega^\beta(0) + \omega^\alpha(0)\omega^\beta(1)) \\
\epsilon^{\alpha\beta}(0) &= \frac{1}{\sqrt{6}}(\omega^\alpha(-1)\omega^\beta(1) + 2\omega^\alpha(0)\omega^\beta(0) + \omega^\alpha(1)\omega^\beta(-1)) \\
\epsilon^{\alpha\beta}(-1) &= \frac{1}{\sqrt{2}}(\omega^\alpha(0)\omega^\beta(-1) + \omega^\alpha(-1)\omega^\beta(0)) \\
\epsilon^{\alpha\beta}(-2) &= \omega^\alpha(-1)\omega^\beta(-1)
\end{aligned} \tag{15}$$

The helicity ratios are introduced as

$$x^2 = \frac{|a_1|^2}{|a_0|^2} \text{ and } y^2 = \frac{|a_2|^2}{|a_0|^2},$$

where a_λ , $\lambda = 0, 1, 2$, are the normalized helicity amplitudes, which satisfy $|a_0|^2 + |a_1|^2 + |a_2|^2 = 1$. Namely, $|a_\lambda|^2$ is the probability of the final state meson with helicity $\pm\lambda$. Then the ratios x^2 and y^2 only depend on the mass ratio m_c/m_b . With the same choice of parameters, we predict ratios for different helicities in Table II.

III. RADIATIVE DECAYS OF HEAVY QUARKONIUM INTO LIGHT MESONS

As a purely phenomenological model-dependent study, In this section we will extend our calculations performed above for radiative decays of bottomonia into charmonia to the radiative decays of bottomonia into light mesons. Our assumption is that the light mesons such as the $f_2(1270)$, $f'_2(1525)$, and $f_1(1285)$ can be described by nonrelativistic $q\bar{q}$ ($q = u, d, s$) bound states with constituent quark masses.

In the numerical calculations, the light quark masses are taken to be $m_s = 0.50$ GeV, $m_u = m_d = 0.35$ GeV. The parameters for the heavy quarks are the same as that used in section II, $|\mathcal{R}_S^{bb}(0)|^2 = 6.477$ GeV³, $|\mathcal{R}_S^{cc}(0)|^2 = 0.81$ GeV³, $|\mathcal{R}_P^{bb}(0)|^2 = 1.417$ GeV⁵, $|\mathcal{R}_P^{cc}(0)|^2 = 0.075$ GeV⁵, $m_b = 4.7$ GeV, and $m_c = 1.5$ GeV. The strong coupling constant is chosen as $\alpha_s = 0.19$ and $\alpha_s = 0.26$ in bottomonium and charmonium decays respectively.

As widely accepted assignments we assume that $f_2(1270)$ and $f_1(1285)$ are mainly composed of $(u\bar{u} + d\bar{d})/\sqrt{2}$ (neglecting the mixing with $s\bar{s}$ for simplicity). But for $f_0(980)$, there are many possible assignments such as the tetraquark state, the $K\bar{K}$ molecule, and the P-wave $s\bar{s}$ dominated state (for related discussions on $f_0(980)$ and other scalar mesons, see, e.g., the topical review–note on scalar mesons in [14] and [19]). Since experimental data show that $D_s^+ \rightarrow f_0(980)\pi^+$ has a large branching ratio (BR)[14], here we assign $f_0(980)$ as an $s\bar{s}$ dominated P-wave state as a tentative choice (we do not try to justify this assignment).

As to the wave functions at the origin of light mesons, it is very difficult to determine them without any doubt. Using the theoretical expression for the widths of $f_2 \rightarrow \gamma\gamma$ [1],

$$\begin{aligned}
\Gamma_{f_2(1270) \rightarrow \gamma\gamma}^{(th)} &= \frac{6N_c}{5}(Q_u^2 + Q_d^2)^2 \alpha^2 \frac{|\mathcal{R}'_P(0)|^2}{m^4} \left(1 - \frac{8\alpha_s}{3\pi}\right)^2 \\
\Gamma_{f'_2(1525) \rightarrow \gamma\gamma}^{(th)} &= \frac{12N_c}{5} Q_s^4 \alpha^2 \frac{|\mathcal{R}'_P(0)|^2}{m^4} \left(1 - \frac{8\alpha_s}{3\pi}\right)^2,
\end{aligned} \tag{16}$$

where $N_c=3$ is the color number, $\alpha = 1/137$, and fitting them with their experimental values 2.6 KeV and 0.081 KeV for $f_2(1270)$ and $f'_2(1525)$ respectively[14], we get

$$\begin{aligned}
|\mathcal{R}'_P^{n\bar{n}}(0)|^2 &= 1.58 \times 10^{-3} \text{ GeV}^5, \\
|\mathcal{R}'_P^{s\bar{s}}(0)|^2 &= 2.23 \times 10^{-3} \text{ GeV}^5.
\end{aligned} \tag{17}$$

process	$\Upsilon \rightarrow \gamma f_0(n\bar{n})$	$\Upsilon \rightarrow \gamma f_1(1285)$	$\Upsilon \rightarrow \gamma f_2(1270)$	$\Upsilon \rightarrow \gamma f_0(980)$	$\Upsilon \rightarrow \gamma f_1'(1420)$	$\Upsilon \rightarrow \gamma f_2'(1525)$
BR_{th}^{QCD}	7.2×10^{-5}	2.6×10^{-5}	7.1×10^{-5}	2.2×10^{-5}	1.0×10^{-5}	2.2×10^{-5}
$BR_{th}^{QCD+QED}$	6.4×10^{-5}	3.9×10^{-5}	6.3×10^{-5}	2.0×10^{-5}	1.2×10^{-5}	2.0×10^{-5}
BR_{ex}	\	\	$1.00 \pm 0.10 \times 10^{-4}$	$< 3 \times 10^{-5}$	\	$3.7_{-1.1}^{+1.2} \times 10^{-5}$
process	$J/\psi \rightarrow \gamma f_0(n\bar{n})$	$J/\psi \rightarrow \gamma f_1(1285)$	$J/\psi \rightarrow \gamma f_2(1270)$	$J/\psi \rightarrow \gamma f_0(980)$	$J/\psi \rightarrow \gamma f_1'(1420)$	$J/\psi \rightarrow \gamma f_2'(1525)$
BR_{th}^{QCD}	2.0×10^{-3}	2.0×10^{-3}	2.5×10^{-3}	6.7×10^{-4}	7.5×10^{-4}	8.5×10^{-4}
$BR_{th}^{QCD+QED}$	1.8×10^{-3}	2.7×10^{-3}	2.4×10^{-3}	6.5×10^{-4}	8.5×10^{-4}	8.5×10^{-4}
BR_{ex}	\	$(6.1 \pm 0.8) \times 10^{-4}$	$(13.8 \pm 1.4) \times 10^{-4}$	\	$(7.9 \pm 1.3) \times 10^{-4}$	$(4.5_{-0.4}^{+0.7}) \times 10^{-4}$

TABLE III: Numerical results for $\Upsilon(J/\psi) \rightarrow \gamma f_J$.

If we use the leading order formula in Eq(16), then

$$\begin{aligned} |\mathcal{R}_P^{m\bar{n}}(0)|^2 &= 6.6 \times 10^{-4} \text{ GeV}^5 \\ |\mathcal{R}_P^{s\bar{s}}(0)|^2 &= 1.1 \times 10^{-3} \text{ GeV}^5. \end{aligned} \quad (18)$$

For the vector mesons, the wave functions at the origin may be determined from their leptonic decay $V \rightarrow e^+e^-$ ($V = \phi, \rho$) widths. Using

$$\Gamma(\phi(1020) \rightarrow e^+e^-) = N_c Q_s^2 \alpha^2 \frac{|\mathcal{R}(0)|^2}{3m_s^2} \left(1 - \frac{8\alpha_s}{3\pi}\right)^2 = (1.27 \pm 0.04) \text{ KeV}, \quad (19)$$

we can get

$$\begin{aligned} |\mathcal{R}_S^{n\bar{n}}(0)|^2 &= 0.11 \text{ GeV}^3, \\ |\mathcal{R}_S^{s\bar{s}}(0)|^2 &= 0.19 \text{ GeV}^3. \end{aligned} \quad (20)$$

If we use the leading order formula in Eq.(19), then

$$\begin{aligned} |\mathcal{R}_S^{n\bar{n}}(0)|^2 &= 0.032 \text{ GeV}^3, \\ |\mathcal{R}_S^{s\bar{s}}(0)|^2 &= 0.054 \text{ GeV}^3. \end{aligned} \quad (21)$$

The wave functions at the origin of light mesons can also be determined from potential models [20]. From experimental data, $\Delta E = M(2S) - M(1S)$ is 675 MeV, 638 MeV, 661 MeV, 589 MeV, and 563 MeV for ρ , ω , ϕ , J/ψ , and Υ respectively. In the logarithmic potential, ΔE is independent of quark masses. So we may select the logarithmic potential, which gives

$$\begin{aligned} |R_S(0)|^2 &\propto m_q^{3/2} \\ |R_P(0)|^2 &\propto m_q^{5/2} \end{aligned} \quad (22)$$

With $|\mathcal{R}_S^{c\bar{c}}(0)|^2 = 0.81 \text{ GeV}^3$ and $|\mathcal{R}_P^{c\bar{c}}(0)|^2 = 0.075 \text{ GeV}^5$ ¹. Then we can get

$$\begin{aligned} |\mathcal{R}_S^{n\bar{n}}(0)|^2 &= \left(\frac{m_n}{m_c}\right)^{3/2} |\mathcal{R}_S^{c\bar{c}}(0)|^2 = 0.091 \text{ GeV}^3 \\ |\mathcal{R}_S^{s\bar{s}}(0)|^2 &= \left(\frac{m_s}{m_c}\right)^{3/2} |\mathcal{R}_S^{c\bar{c}}(0)|^2 = 0.156 \text{ GeV}^3 \\ |\mathcal{R}_P^{m\bar{n}}(0)|^2 &= \left(\frac{m_n}{m_c}\right)^{5/2} |\mathcal{R}_P^{c\bar{c}}(0)|^2 = 1.97 \times 10^{-3} \text{ GeV}^5 \\ |\mathcal{R}_P^{s\bar{s}}(0)|^2 &= \left(\frac{m_s}{m_c}\right)^{5/2} |\mathcal{R}_P^{c\bar{c}}(0)|^2 = 4.81 \times 10^{-3} \text{ GeV}^5 \end{aligned} \quad (23)$$

¹ The wavefunction at the origin in the logarithmic potential for $c\bar{c}$ is $|\mathcal{R}_S^{c\bar{c}}(0)|^2 = 0.815 \text{ GeV}^3$ and $|\mathcal{R}_P^{c\bar{c}}(0)|^2 = 0.078 \text{ GeV}^5$. It is consistent with the B-T potential result that was used here.

process	$\chi_{b2} \rightarrow \gamma\rho$	$\chi_{b1} \rightarrow \gamma\rho$	$\chi_{b0} \rightarrow \gamma\rho$	$\eta_b \rightarrow \gamma\rho$
$\Gamma_{QCD}(\text{GeV})$	1.1×10^{-10}	2.2×10^{-10}	3.5×10^{-11}	1.2×10^{-10}
$\Gamma_{QCD+QED}(\text{GeV})$	6.8×10^{-10}	2.2×10^{-10}	8.4×10^{-10}	1.1×10^{-8}
process	$\chi_{b2} \rightarrow \gamma\omega$	$\chi_{b1} \rightarrow \gamma\omega$	$\chi_{b0} \rightarrow \gamma\omega$	$\eta_b \rightarrow \gamma\omega$
$\Gamma_{QCD}(\text{GeV})$	1.2×10^{-11}	2.4×10^{-11}	3.8×10^{-12}	1.3×10^{-11}
$\Gamma_{QCD+QED}(\text{GeV})$	7.6×10^{-11}	2.4×10^{-11}	9.3×10^{-11}	1.2×10^{-9}
process	$\chi_{b2} \rightarrow \gamma\phi$	$\chi_{b1} \rightarrow \gamma\phi$	$\chi_{b0} \rightarrow \gamma\phi$	$\eta_b \rightarrow \gamma\phi$
$\Gamma_{QCD}(\text{GeV})$	3.6×10^{-11}	5.8×10^{-11}	1.6×10^{-11}	5.9×10^{-11}
$\Gamma_{QCD+QED}(\text{GeV})$	1.3×10^{-10}	5.8×10^{-11}	7.5×10^{-11}	1.2×10^{-9}
process	$\chi_{c2} \rightarrow \gamma\rho$	$\chi_{c1} \rightarrow \gamma\rho$	$\chi_{c0} \rightarrow \gamma\rho$	$\eta_c \rightarrow \gamma\rho$
BR_{th}^{QCD}	1.3×10^{-5}	4.1×10^{-5}	3.2×10^{-6}	1.5×10^{-6}
$BR_{th}^{QCD+QED}$	3.8×10^{-5}	4.2×10^{-5}	2.0×10^{-6}	4.5×10^{-6}
process	$\chi_{c2} \rightarrow \gamma\omega$	$\chi_{c1} \rightarrow \gamma\omega$	$\chi_{c0} \rightarrow \gamma\omega$	$\eta_c \rightarrow \gamma\omega$
BR_{th}^{QCD}	1.5×10^{-6}	4.6×10^{-6}	3.5×10^{-7}	1.7×10^{-7}
$BR_{th}^{QCD+QED}$	4.2×10^{-6}	4.7×10^{-6}	2.2×10^{-7}	5.0×10^{-7}
process	$\chi_{c2} \rightarrow \gamma\phi$	$\chi_{c1} \rightarrow \gamma\phi$	$\chi_{c0} \rightarrow \gamma\phi$	$\eta_c \rightarrow \gamma\phi$
BR_{th}^{QCD}	3.3×10^{-6}	1.1×10^{-5}	1.3×10^{-6}	7.1×10^{-7}
$BR_{th}^{QCD+QED}$	6.5×10^{-6}	1.1×10^{-5}	3.0×10^{-8}	4.0×10^{-7}

TABLE IV: Predicted decay widths for $\chi_{bJ}(\eta_b) \rightarrow \gamma\rho(\omega, \phi)$.

$m_q(\text{GeV})$		QCD	QCD+QED		QCD	QCD+QED		QCD	QCD+QED
0.35	$x^2(\Upsilon \rightarrow \gamma f_2)$	0.023	0.023	$y^2(\Upsilon \rightarrow \gamma f_2)$	0.0013	0.0014	$x^2(\Upsilon \rightarrow \gamma f_1)$	0.00069	0.00010
0.635	$x^2(\Upsilon \rightarrow \gamma f_2)$	0.073	0.075	$y^2(\Upsilon \rightarrow \gamma f_2)$	0.0095	0.010	$x^2(\Upsilon \rightarrow \gamma f_1)$	0.0047	0.0067
0.50	$x^2(\Upsilon \rightarrow \gamma f_2')$	0.045	0.046	$y^2(\Upsilon \rightarrow \gamma f_2')$	0.0043	0.0045	$x^2(\Upsilon \rightarrow \gamma f_1')$	0.0018	0.0023
0.763	$x^2(\Upsilon \rightarrow \gamma f_2')$	0.10	0.11	$y^2(\Upsilon \rightarrow \gamma f_2')$	0.017	0.018	$x^2(\Upsilon \rightarrow \gamma f_1')$	0.0087	0.010
0.35	$x^2(J/\psi \rightarrow \gamma f_2)$	0.21	0.21	$y^2(J/\psi \rightarrow \gamma f_2)$	0.055	0.057	$x^2(J/\psi \rightarrow \gamma f_1)$	0.026	0.029
0.635	$x^2(J/\psi \rightarrow \gamma f_2)$	0.62	0.62	$y^2(J/\psi \rightarrow \gamma f_2)$	0.33	0.33	$x^2(J/\psi \rightarrow \gamma f_1)$	0.13	0.14
0.50	$x^2(J/\psi \rightarrow \gamma f_2')$	0.40	0.40	$y^2(J/\psi \rightarrow \gamma f_2')$	0.16	0.16	$x^2(J/\psi \rightarrow \gamma f_1')$	0.072	0.074
0.763	$x^2(J/\psi \rightarrow \gamma f_2')$	0.86	0.86	$y^2(J/\psi \rightarrow \gamma f_2')$	0.57	0.57	$x^2(J/\psi \rightarrow \gamma f_1')$	0.21	0.22

TABLE V: Results for $\Upsilon \rightarrow \chi_{cJ}\gamma$ with different helicity states

In the numerical calculation, the parameters are taken to be $|\mathcal{R}_S^{s\bar{s}}(0)|^2 = 0.054 \text{ GeV}^3$, $|\mathcal{R}_S^{n\bar{n}}(0)|^2 = 0.032 \text{ GeV}^3$, $|\mathcal{R}_P^{s\bar{s}}(0)|^2 = 1.1 \times 10^{-3} \text{ GeV}^5$, $|\mathcal{R}_P^{n\bar{n}}(0)|^2 = 6.6 \times 10^{-4} \text{ GeV}^5$. The numerical results are shown in Table III and Table IV.

The branching ratio of Υ radiative decay into a light meson is smaller than the corresponding branching ratio of J/ψ by a factor of

$$\frac{BR(\Upsilon \rightarrow \gamma M)}{BR(J/\psi \rightarrow \gamma M)} \sim \left(\frac{Q_b}{Q_c}\right)^2 \left(\frac{m_c}{m_b}\right)^2 \frac{\alpha(2m_b)}{\alpha(2m_c)} \sim 0.02 \quad (24)$$

We can find this theoretical ratio is $0.013 \sim 0.036$. The experimental ratio is 0.072 for $f_2(1270)$, and 0.082 for $f_2'(1525)$. The corresponding theoretical ratios are 0.026 and 0.024 for $f_2(1270)$ and $f_2'(1525)$ respectively. If we use larger constituent quark masses, e.g. $m_u = m_d = M(1270)/2$, $m_s = M(1525)/2$, the ratios are 0.018 and 0.018 for $f_2(1270)$ and $f_2'(1525)$ respectively.

With the same parameters, we give the branching ratios for different helicity states in Table V. The corresponding values of helicity parameters x and y are $x = 0.46$, $y = 0.23$. Recently, new experimental data for the contributions of different helicities in process $J/\psi \rightarrow \gamma f_2(1270)$ have been given by the BES Collaboration [?]: $x = 0.89 \pm 0.02 \pm 0.10$ and $y = 0.46 \pm 0.02 \pm 0.17$ (see also[14]). It is about 2 times larger than our results. But if we use a larger constituent quark mass, e.g. $m_u = M(1270)/2$, we will get substantially increased values $x = 0.79$ and $y = 0.58$ (also see Ref.[2]). We emphasize that the helicity parameters are very sensitive to the light quark masses, and hence very useful in clarifying the decay mechanisms. Note that if $m_u/m_c \rightarrow 0$, we will have $x \rightarrow 0$ and $y \rightarrow 0$, but this is inconsistent with data.

IV. SUMMARY

In this paper, we mainly investigate the radiative decays of bottomonium into charmonium, such as $\Upsilon \rightarrow \chi_{cJ}\gamma$, $\chi_{bJ} \rightarrow J/\psi\gamma$, $\eta_b \rightarrow J/\psi\gamma$ and $\Upsilon \rightarrow \eta_c\gamma$ based on the NRQCD approach. Based on our numerical calculations, we predict that the branching ratios of $\Upsilon \rightarrow \chi_{cJ}\gamma$ and decay widths of $\chi_{bJ} \rightarrow J/\psi\gamma$. All the above processes are perturbative calculable, and it is a good way to test NRQCD.

We next focus on the cases of heavy quarkonium radiative decays into light mesons, including $\Upsilon(J/\psi) \rightarrow f_J\gamma$ and $\chi_{bJ} \rightarrow \rho(\omega, \phi)\gamma$ et ac.

In this work, we also find that the QED effects in some radiative processes are really significant. For $\Upsilon \rightarrow \gamma\chi_{cJ}$ decay, the pure electromagnetic process only affects the final results for $J = 0, 2$ a little, but for the $J = 1$ state the result may change by a factor of 2. The same results will be seen in the decays of $\Upsilon \rightarrow \gamma f_J$ and $J/\psi \rightarrow \gamma f_J$. As the cases of χ_{bJ} decays, especially for the process $\chi_{bJ} \rightarrow \rho(\omega, \phi)\gamma$, QED process may give dominant contributions.

Acknowledgments

We would like to thank Ce Meng for valuable discussions. This work was supported in part by the National Natural Science Foundation of China (No 10421503, No 10675003), the Key Grant Project of Chinese Ministry of Education (No 305001), and the Research Found for Doctorial Program of Higher Education of China.

-
- [1] G. T. Bodwin, E. Braaten and G. P. Lepage, Phys. Rev. D **51**, 1125 (1995); **55**, 5853(E) (1997).
 - [2] J.G. Körner, J.H. Kühn, and H. Schneider, Phys. Lett. B **120**, 444 (1983); J.G. Körner, J.H. Kühn, M. Kramer, and H. Schneider, Nucl. Phys. B **229**, 115 (1983).
 - [3] M. Kramer, Phys. Lett. B **74**, 361 (1978); J.G. Körner and M. Kramer, Z. Phys. C **16**, 279 (1983).
 - [4] Y.J. Gao, Y.J. Zhang and K.T. Chao, Chin. Phys. Lett. **23**, 2376 (2003) (hep-ph/0607278).
 - [5] Y.J. Gao, Y.J. Zhang, and K.T. Chao, Commun. Theor. Phys. **46**, 1017 (2006) (hep-ph/0606170).
 - [6] P. Cho and A.K. Leibovich, Phys. Rev. **D53**, 150 (1996); **53**, 6203 (1996); P. Ko, J. Lee and H.S. Song, Phys. Rev. **D54**, 4312 (1996); K.Y. Liu, Z.G. He, K.T. Chao, Phys. Lett. **B557**, 45 (2003).
 - [7] J. H. Kühn, Nucl. Phys. B **157**, 125 (1979); B. Guberina *et al.*, Nucl. Phys. B **174**, 317 (1980).
 - [8] R. Mertig, M. Böhm, A. Denner, Comput. Phys. Commun. **64** (1991) 345.
 - [9] T. Hahn, M. Perez-Victoria, Comput. Phys. Commun. **118** (1999) 153.
 - [10] A. Denner, S. Dittmaier, Nucl.Phys. **B658** (2003) 175; A. Denner, S. Dittmaier, hep-ph/0509141.
 - [11] E.J. Eichten and C. Quigg, Phys. Rev. D **52**, 1726 (1995).
 - [12] J.P. Ma, Nucl. Phys. B **605** 625 (2001); Erratum-ibid. **B611** 523(2001).
 - [13] S. B. Athar *et al.* [CLEO Collaboration], Phys. Rev. D **73**, 032001 (2006) [arXiv:hep-ex/0510015].
 - [14] S. Eidelman, et al. [Particle Data Group], Phys. Lett. B **592** (2004) 1; W. M. Yao *et al.* [Particle Data Group], J. Phys. G **33**, 1 (2006).
 - [15] E. Braaten, S. Fleming, and A.K. Leibovich, Phys. Rev. **D63**, 094006 (2001).
 - [16] F. Maltoni and A.D. Polosa, Phys. Rev. **D70**, 054014 (2004).
 - [17] Y. Jia, hep-ph/0611130.
 - [18] G. Hao, Y. Jia, C.F. Qiao, and P. Sun, hep-ph/0612173.
 - [19] F.E. Close, G.R. Farrar, and Z.P. Li, Phys. Rev. D **55**, 5749 (1997).
 - [20] C. Quigg and J. L. Rosner, Phys. Rept. **56**, 167 (1979).